

# Force generation in small ensembles of Brownian motors

Martin Lindén,\* Tomi Tuohimaa,† and Mats Wallin‡

*Department of Physics, Royal Institute of Technology (KTH), AlbaNova, 10691 Stockholm, Sweden*

Ann-Beth Jonsson

*Department of Medical Biochemistry and Microbiology, Uppsala Biomedical Center,  
Uppsala University, Box 582, 75123 Uppsala, Sweden*§

Motility of certain gram-negative bacteria is mediated by retraction of type IV pili surface filaments, which are essential for infectivity. The retraction is powered by a strong molecular motor protein, PilT, producing very high forces that can exceed 100 pN. The molecular details of the motor mechanism are still largely unknown, while other features have been identified recently, such as the ring shaped protein structure of the PilT motor. The surprisingly high forces generated by the PilT motor motivates investigation of generation of large forces in molecular motors. To this end, we study a simple model, inspired by the known features of the PilT motor, involving a small ensemble of coupled motor units in a ring shaped arrangement. The model describes the motor units in terms of elastically coupled particles in an asymmetric, time dependent binding potential (flashing ratchet potential), corresponding to the ATP hydrolysis cycle. We compute the stall force and force velocity relations in a subset of the parameter space, and find that the maximum force (stall force) is determined by a competition between three different mechanisms, depending on coupling, binding strength, and ensemble size. Compared with its constituents without coupling, we find higher efficiency and qualitatively different force-velocity relationships. The model captures several of the qualitative features obtained in recent experiments on pilus retraction forces, such as a plateau in velocity at low loads and insensitivity in the stall force to changes in ATP concentration.

PACS numbers: 05.40.-a,87.16.-b

## I. INTRODUCTION

Recent experimental progress has enabled remarkable quantitative measurement of biological processes on single molecule level [1]. One example is the biomechanics of force generation by molecular machines such as kinesin, myosin, and dynein [2, 3]. This has stimulated considerable modeling activity in order to analyze the experiments [4, 5, 6, 7]. In this paper we are inspired by another molecular motor, the recently discovered PilT motor [8], whose detailed function is unknown but has interesting properties, e.g., it is the strongest known linear motor protein.

The PilT motor is responsible for retraction of certain bacterial surface filaments, and the velocities and forces generated during retraction events was recently measured in a series of laser tweezer experiments [9, 10, 11]. Theoretical analysis of retraction data can reveal interesting information about the underlying retraction mechanism [11, 12], but one is also led to the more fundamental question of how large the generated forces can be, given the energy- and length scales relevant to the PilT motor, and what features are important for generation of large forces. We will address this question through a simple ratchet model, which is inspired by known experimental

facts about the PilT system.

Ratchet models of particles in fluctuating potentials are commonly used in the theory of molecular motors [4, 13]. Single particle models have been used to study kinetics of ATP-consumption in molecular motors [14], and to describe kinetics of kinesin [15]. Models of particles in ratchet potentials have also been employed to describe collective effects in large ensembles of interacting motors [16, 17, 18, 19, 20, 21]. Finite ensembles of Brownian particles have been studied to some extent in the context of two-headed motor proteins, using extended models [7, 22, 23].

In this paper, we investigate the behavior of a small processive ensemble of coupled Brownian motors and focus on the effect of coupling, and on generation of large forces. We aim at a prototypical, minimal model which captures interesting features of the experimental results. The main input are the overall structures of the filament and PilT complex. When possible, we also use the experimental situation to estimate model parameters, which should ideally be as few as possible. The model is a generalization of the model of coupled correlated motors studied in Ref. [24] to finite ensembles, but we study different properties. By exploring the parameter space of coupling and binding to the filament, we will see how those factors limit the generation of large forces in different parameter regimes. We compare with a single building block of our model to better understand the effect of coupling, and also compare with experimental results. Although the detailed connection between the model and the actual molecular retraction mechanism is speculative,

\*Electronic address: linden@kth.se

†Electronic address: tomi.tuohimaa@biox.kth.se

‡Electronic address: wallin@kth.se

§Electronic address: Ann-Beth.Jonsson@imbim.uu.se

the spirit of the model is best understood in light of the known facts about the TFP system. Therefore, we will briefly review some facts about pilus retraction, before introducing the model.

PilT is a motor protein required for retraction of type IV pili (TFP). TFP are surface filaments crucial for initial adherence of certain gram-negative bacteria to target host cells, DNA uptake, cell signalling, and bacterial motility [8]. The pili filaments consist of thousands of pilin subunits that polymerize to helical filaments with outer diameter of about 6 nm, a 4 nm pitch and 5 subunits per turn [8, 25]. The bacterial motility associated with TFP, called twitching motility, is driven by repeated extension, tip attachment, and retraction of TFP, by which the bacterium can pull itself forward on surfaces like glass plates or target host cells [9]. TFP are expressed by a wide range of gram-negative bacteria [8] including *Myxococcus xanthus* [26] and human pathogens *Neisseria gonorrhoeae* [9] and *Pseudomonas aeruginosa* [27].

The mechanism of retraction is believed to be filament disassembly mediated by PilT, a member of the AAA family of motor proteins [8, 28]. Retraction is highly processive, and retraction velocities are of order  $0.5 - 1 \mu\text{m/s}$  [8, 10, 11, 27]. Generation of high forces persists when the PilT concentration is reduced, suggesting that one single PilT complex retracts the pilus filament [10]. The stall force and high load velocity is insensitive to changes in ATP-concentration, and the retraction velocity is load-independent for small loads ( $\lesssim 50 \text{ pN}$ ) [10, 11]. PilT has been shown to form a ring structure with 6-fold symmetry. One possibility is that it can hydrolyze up to 6 ATP molecules in parallel during retraction [8, 10]. The outer diameter of the ring is about 10 nm, and the inner diameter varies in the range 2-4 nm [29].

TFP retraction is interesting from a technological point of view, as a prototype for a nano-machine that can generate large forces, and from a biomedical point of view since pilus retraction is important for the infectivity of various severe bacterial pathogens [30].

There are several proposals for the molecular details of the retraction mechanisms [8], and one of them is that PilT forms a ring around the base of the pilus [8, 31]. The hole in the middle of the PilT complex seems too small to let the assembled filament through, but large enough for pilin subunits. This could allow interactions between the pilus and PilT via several active sites (subunits) that work together, and is the principle which we will explore here. The basic setup is sketched in Fig. 1A, where  $q$  is the retraction coordinate. We also allow for small deformations of the protein through displacements  $x_i$  of the subunits from their equilibrium positions. If we assume that the subunits interact with the filament strands via effectively one-dimensional potentials, the helical setup in Fig. 1A can be mapped to a simpler geometry. This equivalent geometry is one where the motors all move in the same potential (but do not interact directly with each other). To reflect the relative displacement of the different filament strands, the equilibrium positions of

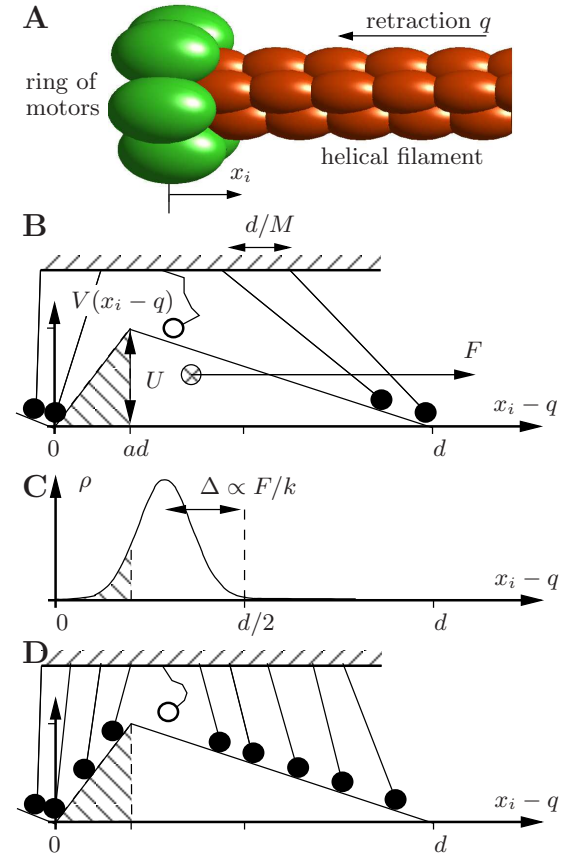


Figure 1: (A) Elements of the retraction motor model. (B) Equivalent geometry: Non-interaction particles in ratchet potential are elastically coupled to a stiff backbone. Open circles represent particles which do not interact with the ratchet potential. The equilibrium positions of the particles are placed evenly over one period of the potential. During retraction, the filament (and hence the potential) moves to the left, so the external load  $F$  is defined as positive when opposing retraction. The potential has amplitude  $U$ , which measures the binding strength of the subunits to the filament, and we use  $a = 0.1$  for the asymmetry. (C) Distribution of a free subunit. Dashed area represents the chance to bind to the rear potential well (failed step). As the load increases, the distribution is pulled backwards from the  $F=0$  equilibrium centered at  $d/2$ . (D) With many motor subunits and strong coupling, some motors will bind to the left part of the potential and contribute negatively to the stall force. This means that for many motors and given binding strength  $U$ , maximal stall force is obtained for some finite coupling  $k_{\text{opt}}$ . In the case of few motors, the stall force is an increasing function of  $k$ .

the subunits are spread evenly over one period, as shown in Fig. 1B, which is the picture we will use. Except for a different implementation of the coupling and drag coefficients, our model is a generalization of [24] to more motor subunits and, most important, an external load.

We stress that the purpose of this paper is not to attempt to describe the detailed molecular mechanisms

involved in pilus retraction, which is largely unknown. Rather we examine a new regime of a simple model, whose main features are inspired by recent experiments. Below we obtain several attractive results from the model, such as large force generation and other properties that agree well with experimental results on pilus retraction. Moreover, these results are a consequence of coupling and correlation between the subunits, and strikingly different from the characteristics of the single building block of the model.

## II. THE MODEL

We formulate the retraction dynamics as a system of over-damped Langevin equations for  $q$  and  $x_i$ , as illustrated in Fig. 1B. The equations of motion are

$$\begin{aligned} \alpha \dot{x}_j &= -k(x_j - \frac{jd}{M}) - h_j(t) \frac{\partial V(x_j)}{\partial x_j} + \sqrt{2\alpha k_B T} \xi_j(t) \\ \gamma \dot{q} &= \sum_{j=1}^M h_j(t) \frac{\partial V(x_j)}{\partial x_j} + F + \sqrt{2\gamma k_B T} \xi_0(t) \end{aligned} \quad (1)$$

where  $j = 1, \dots, M$ .  $\alpha$  and  $\gamma$  are friction coefficients of the internal subunits and the filament respectively,  $k$  is a spring constant,  $h_j(t)$  are bond state variables,  $V$  is the binding potential between the filament and the motor subunits as shown in Fig. 1B,  $k_B$  is Boltzmann's constant,  $T$  is the temperature,  $F$  is an external load acting on the filament, and  $M$  is the number of motor subunits.  $\xi_j(t)$  are independent Gaussian white noise processes with  $\langle \xi_j(t) \rangle = 0$ ,  $\langle \xi_i(t) \xi_j(t') \rangle = \delta_{ij} \delta(t - t')$  and prefactors according to the fluctuation-dissipation theorem. The temperature is set to  $T = 310$  K.

In the model the motor subunits can be in one of two states: Free ( $h_j = 0$ ) in which they diffuse around an equilibrium position, or bound ( $h_j = 1$ ), in which they bind to the pilus filament through the potential  $V(x_j)$ . The pilus filament is composed of pilin subunits arranged in a helical conformation, with 4 nm pitch and 5 subunits per turn [8, 25]. To mimic this structure, we take the potentials to be periodic with period  $d = 4$  nm, and the equilibrium positions of the motor subunits to be spatially displaced over one period of the potential.

The number of subunits  $M$  is a parameter, and we will present results for  $M = 2, 3, 5, 6$  and 12. We model the binding of the motor to the filament by an asymmetric sawtooth potential shown in Fig. 1C. Some asymmetry is needed to give a preferred direction of motion, and the sawtooth potential was selected to give a simple parameterization of the real interaction potential, whose form is unknown. One realization of a sawtooth-like potential is interaction with polar monomers [2], which is consistent with the hydrophilic character of the pilin subunit. Alternatively, it can be viewed as an effective description of asymmetry elsewhere in the system, e.g., in the direction

of the motor steps (power strokes). The exact implementation is not expected to influence the overall qualitative features of the model.

Details of the potential shape are smoothed out by the thermal noise, and are not critical for our results. The amplitude  $U$  of the potential is the maximal energy required to break the bond between the filament and the active site. Pilus retraction is powered by hydrolysis of one or a few ATP per pilin subunit [10], which sets the energy scale for the potential: Depending on conditions, the energy yield from hydrolysis of one ATP in a cell is about 80 pN nm [2, 3]. The motor units are located in the PilT region, and we model their confinement with a harmonic restoring force  $-k(x_j - jd/M)$ . For the bonding processes  $h_j(t)$ , we restrict ourselves to an  $M$ -state model, where the  $j$ :th state is defined by  $h_k(t) = 1 - \delta_{kj}$ . The states are visited in ascending order, and the (constant) transition rate is  $\lambda$ . This irreversibility agrees with an analysis of pilus retraction in terms of a chemical rate model, which indicates that there are practically irreversible sub-steps in the retraction cycle [12]. This bonding scheme results in retraction as subunits are released from one potential well, while their equilibrium positions are in the potential well one step ahead. The subunits are therefore pulled over the potential barrier before they bind in again. This mechanism relies on the asymmetry of the potential, and is similar to the mechanisms studied earlier for two coupled particles [24, 32].

In the laser tweezer experiments [9, 10, 11], the filament is attached to a latex bead, with diameter  $1 - 2 \mu\text{m}$ . Using Stokes law,  $\gamma = 6\pi\eta R$ , the approximate viscosity  $\eta = 10^{-8}$  pN s/nm $^2$  of the surrounding protein solution (somewhere between  $10^{-9}$  (water) and  $8.3 \cdot 10^{-7}$  (glycerin) seems reasonable) and  $R = 1 \mu\text{m}$ , we get  $\gamma \approx 2 \cdot 10^{-4}$  pN s/nm for the bead. As a first approximation, we neglect elasticity and friction of the pilus filament itself. For the internal friction coefficient, we use  $\alpha = 0.5 \cdot 10^{-3}$  pN s/nm  $\ll k/\lambda$ . This sets the timescale for internal relaxation  $\alpha/k$  much smaller than the typical time  $\lambda^{-1}$  between transitions, and lets the subunits reach equilibrium between transitions. In this quasi-static region, we expect the velocity to be proportional to  $\lambda$  and the stall force to be independent of  $\lambda$ .

## III. RESULTS

### A. Methods

Retraction of the filament means that  $q$  decreases, so it is natural to study the retraction velocity  $v = -dq/dt$ . In the laser tweezer experiment, the tip of the bead is held by a static laser trap which is to good approximation a harmonic potential, i.e.  $F = -k_t q$ , with  $k_t$  on the order of 0.1 pN/nm. Numerical solution of Eq. (1) using the Milstein scheme [33] produces a deflection trajectory similar to the experimental ones. We calculate the retraction velocity by fitting a second order poly-

nomial to a time interval of width 0.1 s around a point  $q = -F/k_t$ , and taking the velocity  $v(F)$  as the derivative of the polynomial at that point. This is similar in spirit to how the experimental data was analyzed [9, 10, 11], and the details of the analysis do not influence the results significantly (not shown). The retracted distance  $-q(t)$  increases from the initial value towards a steady state, corresponding to the maximal applied force (stall force), which we define as the mean applied force in the steady state.

### B. Stall force and force-velocity relation

In the case of a few motor subunits, stalling of the retraction occur by two different mechanisms. One comes from the finite binding energy between filament and motor, which gives an upper bound of  $U(M-1)/d(1-a)$  for the stall force in absence of noise and elasticity. Thermal noise makes the subunits diffuse over the energy barriers at lower loads. The other has to do with the elastic couplings between a subunit and its equilibrium position. Weak coupling also lowers the stall force, as illustrated in Fig. 1C: With increasing load, the distribution of the free subunit is pulled backwards and the probability of bonding to the right potential well decreases. The width of the distribution of the free subunit is  $\sqrt{k_B T/k}$ , but since the filament also fluctuates, the distribution of the relative coordinate  $x_i - q$  is wider than that. For small  $k$ , the oscillations of the free subunit dominates, the distribution in Fig. 1C is broad, and the deflection  $\Delta$  is large. This means that even a small external force decreases the probability of a successful power stroke, and we see a monotonically decreasing velocity as a function of external load. For large  $k$  we expect the shaded area in Fig. 1C to be small since the distribution is narrow and  $\Delta$  is small. The success rate and hence the velocity is then independent of applied load for small loads, and the stall force is limited by the bonding energy  $U$ . Taken together, these effects will tend to increase the stall force with increased coupling. Figure 2 shows examples of typical normalized force-velocity relations of the model for strong, intermediate and weak coupling  $k$ , compared to the binding strength  $U$ . In general, the stall force is insensitive to changes in the reaction rate  $\lambda$  (not shown), corresponding to different ATP concentrations, as seen experimentally. Stiff systems ( $k/U \gtrsim 1.5/d$ ) have a plateau in the retraction velocity at low load, which is seen in experiments [10, 11].

For large  $M$ , strong coupling has a an additional destructive effect on stall force, as illustrated in Fig. 1D: With strong coupling, the motor subunits will tend to be less displaced from their equilibrium positions. If the distance between equilibrium positions is smaller than the part of the potential with backward slope (dashed), then some of the bound subunits will tend to be in that region, were they act with a negative force on the filament and contribute negatively to the stall force. This

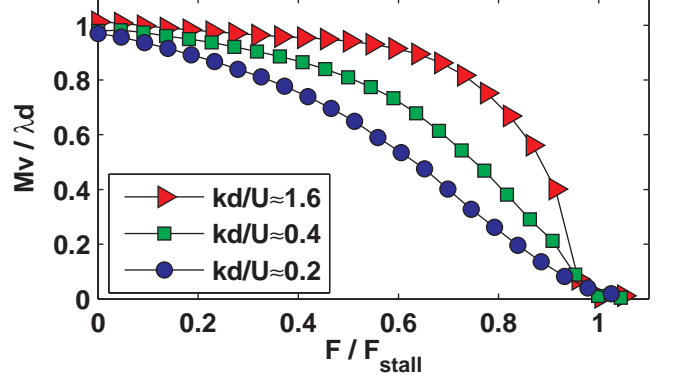


Figure 2: Typical force velocity relations for strong (upper), intermediate (middle) and weak coupling (lower). Calculated for  $M = 5$ . The y-axis is velocity normalized by  $\lambda d/M$ , the ideal velocity for  $M$  motors.  $d = 4$  nm is the potential period, introduced to make the ratio  $kd/U$  dimensionless.

effect is enhanced by increased coupling  $k$ , and so for  $M \gtrsim 1/(1-a) = 10$ , we expect the stall force to a maximum for some optimal coupling.

A parameterization of the stall force is obtained from the following ansatz, which attempts to describe the effect of coupling with an (unknown) function  $f_M(kd/U)$ :

$$F_{\text{stall}}(k, U) = F_{\text{inf}} f_M\left(\frac{dk}{U}\right), \quad F_{\text{inf}} = \frac{M-1}{d(1-a)}(U - U_0) \quad (2)$$

where  $U_0$  is a free parameter, independent of  $U$  and  $k$ . If the ansatz is good, data for different parameters should collapse to a single curve if one plots  $f_M(kd/U) = F_{\text{stall}}/F_{\text{inf}}$  against  $kd/U$  for the correct value of  $U_0$ . Figure 3A shows such a plot with best fit values of  $U_0$ : the parameterization is quite accurate for few motor subunits ( $M = 2, 3, 5$  and  $6$ ), while the collapse is not so good for  $M = 12$ . Heuristically, one can think of  $F_{\text{inf}}$  as the stall force in the stiff limit  $k \rightarrow \infty$ , and  $U_0$  as the effect of thermal fluctuations, that make the motor subunits diffuse over barriers in the potential, thus lowering the maximal force that the binding potential can support.  $f_M(kd/U)$  is a normalized stall force that describes the effect of elasticity, and  $d = 4$  nm was included in the argument to make it dimensionless. As indicated above, one expects  $f_M(x)$  to be an increasing function of  $x$  for small values of  $M$ , since stronger coupling decreases the probability that the free subunit binds to the wrong potential well. For large  $M$ ,  $f_M(x)$  is expected to have a maximum if the ansatz is still valid, due to the high motor density. These expectations are consistent with in Fig. 3, where  $f_2(x)$ ,  $f_3(x)$ ,  $f_5(x)$  and  $f_6(x)$  are monotonically increasing in the simulated region, whereas  $f_{12}(x)$  has a maximum around 1.5, though the collapse is not as good as for lower  $M$ .

The stiff limit  $k \rightarrow \infty$  can be simulated by locking the subunits to their equilibrium positions, and the results are shown in Fig. 3B. Except for  $M = 12$ , the result is

consistent with the above interpretation of the parameterization of Eq. (2) if we set  $f_M(\infty) = 1$ . The values of  $U_0$  obtained from fitting the stall force simulations of the stiff limit to a straight line are within 10 % of the best fit values from the collapse at finite coupling (Fig. 3A). The case  $M = 12$  still gives a straight line for the stall force in the stiff limit, but with a lower slope than  $(M-1)/d(1-a)$ , reflecting the destructive effect of dense subunits in a strongly coupled system with many subunits.

### C. Comparison with single motor model

To further highlight the effect of coupling and correlation, it is interesting to compare the coupled model to its constituents without coupling. This is a single particle in a flashing ratchet potential, and is a special case of the above model, with  $M = 1$  and  $k = \infty$ . The single particle flashing ratchet (SPR) has been studied extensively [4, 34] in different versions, and its properties are qualitatively different from those of the coupled model in several interesting respects. For an SPR in this simple version, the mechanism to pull the particle to the next potential well is not present. Instead, forward motion relies on thermal noise to make the particle diffuse over the barrier while in the unbound state. This means that the probability for a forward step can never exceed 1/2 for a single chemical cycle even at zero external load. With nonzero external load, the free diffusion is superimposed on a backward motion with velocity  $v_{\text{drift}} = -F/\gamma$ , hence the velocity is substantially reduced even at very small loads. These features conspire to make both maximal velocity and stall force depend strongly on the friction constant, the reaction rate, and how much time the particle spends unbound during a reaction cycle [15, 34]. Two typical force velocity relations for SPR is shown in Fig. 4, with 4 nm periodicity,  $U = 160$  pN nm,  $\lambda = 2000$   $s^{-1}$  and damping as above.

### D. Application to a real motor system

In Fig. 4 we compare model results with experimental data on wild type *N. gonorrhoeae*. In this case, there are two natural choices for  $M$ , namely  $M = 5$ , reflecting the 5-fold symmetry of the filament, and  $M = 6$ , reflecting the 6-fold symmetry of the PilT molecule. We present data for  $M = 5$ , but  $M = 6$  is qualitatively no different. The model can describe the average velocity from Ref. [11] to some extent. A qualitative difference is the behavior at very high forces, where the average velocity falls off exponentially [11, 12], while the model results decays faster than that, as seen in Fig. 4. A single retraction event from Ref. [10], has a different decay, and agrees better with the characteristics of the model.

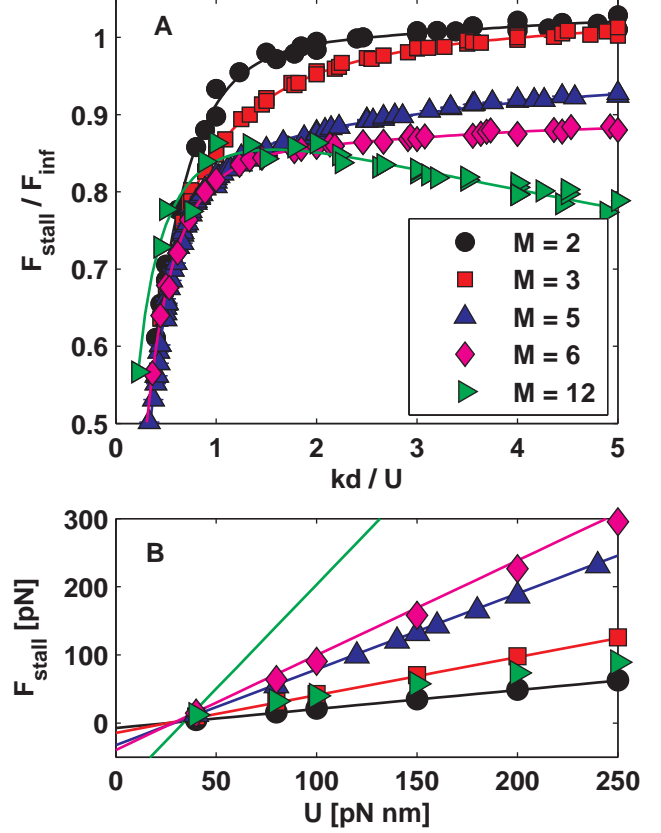


Figure 3: (A) Collapse of stall force dependence on  $k$  and  $U$  using Eq. (2). Data for different parameters collapse approximately to different curves for different number of motor subunits  $M$ , with  $U_0 = 25.4, 25.9, 28.9, 28.3, 33.5$  pN nm for  $M = 2, 3, 5, 6, 12$  respectively. Lines are guides to the eye.  $5 < k < 250$  pN/nm, and  $80 < U < 200$  pN nm. The case of many motors ( $M = 12$ ) is qualitatively different from the other cases, since there is a maximum in the normalised stall force  $f_M(kd/U)$ . When the motors are densely packed (large  $M$ ), and the coupling gets stiff enough, the bound motors will be distributed over all parts of the binding potential. Motors bound on the backward-sloping parts of the potential (dashed area in Fig. 1D) will then give a negative contribution to the stall force, an effect that is enhanced by strong coupling. (B) Stall force in the stiff limit  $k \rightarrow \infty$ . Lines are the stall force of Eq. (2) extrapolated to  $k = \infty$ , assuming  $f_M(\infty) = 1$ , with  $U_0$  as above. For small  $M$ , this extrapolation agree well with best fit lines:  $U_0$  are within 10%, and the slope within 4% (not shown). This is consistent with our interpretation of  $F_{\text{inf}}$  as the stall force in the stiff limit. The deviating line is the extrapolation for  $M = 12$ , which does not describe the simulated results. In this case, the stall force still increases linearly with  $U$ , but with a lower slope than that of Eq. (2). Also, the assumption  $f_{12}(\infty) = 1$  is not valid, as seen in (A). Error bars are smaller than the symbols.

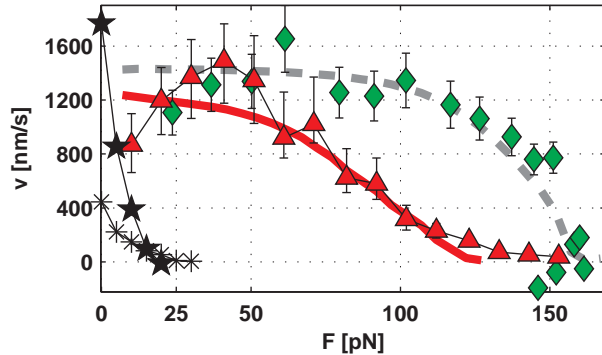


Figure 4: Force-velocity characteristics from simulation and experiment. (Triangles) experimental mean velocity from Ref. [11]. (Full line)  $M = 5$  coupled model,  $U = 200$  pN nm,  $k = 25$  pN/nm,  $F_{\text{stall}} = 122$  pN,  $\lambda = 1600$  s $^{-1}$ . (Diamonds) single retraction event from Ref. [10]. (Dashed line)  $M = 5$  coupled model,  $U = 200$  pN nm,  $k = 60$  pN/nm,  $F_{\text{stall}} = 160$  pN,  $\lambda = 1800$  s $^{-1}$ . Single ratchet models (black) are qualitatively different from the above. We show results for  $M = 1$ ,  $U = 200$  pN nm,  $\lambda = 2000$  s $^{-1}$ ,  $t_{\text{off}} = 25$  ms (\*) and 2.5 ms (\*). Both the mean experimental result and the deviating, single event can be described by the coupled motor model, whereas the single-motor models have quite different characteristics.

#### IV. DISCUSSION AND CONCLUSIONS

We investigate force generation in finite ensembles of coupled molecular motors, inspired by the PilT pilus retraction machinery, the strongest molecular motor reported so far. The model is prototypical, rather than realistic in detail, and offers a possible mechanism for generation of large retraction forces. It includes a ring of elastically coupled motor units, as suggested by the structure of both the PilT protein and the pilus filament, and also contains a few effective parameters describing the local environment. Some parameters can be roughly estimated, and we explore parts of the remaining parameter space and focus on generation of large forces.

We find that the stall force depends on the binding strength  $U$  between motor and filament, the coupling  $k$  between motor subunits, the number of motor subunits  $M$  and an asymmetry parameter. For strong enough coupling we find qualitatively different properties compared to the well studied model of a single particle in a flashing ratchet potential, which are the building blocks of our model. This is not surprising, since the motion of in the single particle model are driven by rectified diffusion, whereas the mechanism for coupled motors are non-diffusive [24, 32]. The dependence of stall force on  $U$ ,  $k$  and  $M$  is well parameterized in an empirical scaling plot (Fig. 3). Weak coupling compared to binding strength has a strong destructive effect on stall force. For few motor subunits, the stall force increases monotonically

with increasing coupling, but when the subunits become dense enough, there is a crossover to different behavior where a strong enough coupling instead has a destructive effect on stall force. For the asymmetry studied here, the crossover occurs around  $M = 10$ .

We compared results from the coupled motor model for the filament retraction force-velocity characteristics with recent experiments on *N. gonorrhoeae*. The coupled model can describe the general features of experimental results, i.e., the plateau in the force-velocity relation at low external loads and the high stall force, which is independent of reaction rate. As seen in Fig. 2, the model generates a family of curves depending on relative coupling strength, from a very marked plateau to an almost linear relation. It is possible that the PilT mechanism performs differently in different conditions and stages of the bacterial life cycle, but it is difficult to tell intrinsic variations from external measurement errors.

Therefore, it makes sense to compare model result both with an average velocity curve from Ref. [11] and a single event from Ref. [10]. Both curves give positive velocities up to around 160 pN, which is in the upper tail of stall forces measured in Ref. [10], but the overall shapes differ. As shown in Fig. 4, the single event seems to be well described for all forces. The averaged curve deviates at high forces, where the experimental mean velocity decays exponentially, which is slower than the model result. The exponential decay can be explained by an Arrhenius law for the rate limiting step at high forces [11, 12]. The present model does not account for such details of the chemical reactions, and in the case of the single trajectory, which is best described, the model is limited mainly by slipping events at high forces. Since the empirical connection between the highly simplified model and the complex biological system is at this stage speculative, it is unclear whether this reflects the underlying behavior of the real system.

Small ensembles of coupled motor systems have previously been found to possess rich behavior without external load [24, 32]. As we have shown, this is true also in the limit of strong load, which is a realistic experimental situation. Generation of strong forces in nano-scale devices is also of technological interest, and it is tempting to speculate about the possibility to realize a setup of coupled motors units pulling on an artificial filament such as a carbon nano tube.

#### Acknowledgments

The authors thank Berenike Maier for valuable discussions and comments. This work was supported by the Swedish Research Council (MW 2003-5001, ABJ 2001-6456, 2002-6240, 2004-4831), the Royal Institute of Technology, the Göran Gustafsson Foundation, the Swedish Cancer Society, and Uppsala University.

---

[1] M. P. Sheetz, ed., *Laser Tweezers in Cell Biology*, vol. 55 of *Methods in Cell Biology* (Academic Press, 1998).

[2] D. Boal, *Mechanics of the Cell* (Cambridge University Press, 2002).

[3] J. Howard, *Mechanics of Motor Proteins and the Cytoskeleton* (Sinauer Associates Inc., 2001).

[4] P. Reimann, Phys. Rep. **361**, 57 (2002).

[5] M. E. Fisher and A. B. Kolomeisky, Proc. Natl. Acad. Sci. **98**, 7748 (2001).

[6] A. B. Kolomeisky and M. E. Fisher, Biophys. J. **84**, 1650 (2003).

[7] I. Derényi and T. Vicsek, Proc. Natl. Acad. Sci. **93**, 6775 (1996).

[8] J. S. Mattick, Annu. Rev. Microbiol. **56**, 289 (2000).

[9] A. J. Merz, M. So, and M. P. Sheetz, Nature **407**, 98 (2002).

[10] B. Maier, L. Potter, M. So, H. S. Seifert, and M. P. Sheetz, Proc. Natl. Acad. Sci. **99**, 16012 (2002).

[11] B. Maier, M. Koomey, and M. P. Sheetz, Proc. Natl. Acad. Sci. USA **101**, 10961 (2004).

[12] M. Lindén, E. Johansson, A.-B. Jonsson, and M. Wallin, (in preparation) (2005), e-Print physics/0504084.

[13] F. Jülicher, A. Ajdari, and J. Prost, Rev. Mod. Phys. **69**, 1269 (1997).

[14] G. Lattanzi and A. Maritan, Phys. Rev. Lett. **86**, 1134 (2001).

[15] R. D. Astumian and M. Bier, Phys. Rev. Lett. **72**, 1766 (1994).

[16] Y. Shu and H. Shi, Phys. Rev. E **69**, 021912 (2004).

[17] M. Badoual, F. Jülicher, and J. Prost, Proc. Natl. Acad. Sci. **99**, 6696 (2002).

[18] T. M. Nieuwenhuizen, S. Klumpp, and R. Lipowsky, Europhys. Lett. **58**, 468 (2002).

[19] F. Jülicher and J. Prost, Phys. Rev. Lett. **75**, 2618 (1995).

[20] F. Jülicher and J. Prost, Phys. Rev. Lett. **78**, 4510 (1997).

[21] Y. Aghababaie, G. I. Menon, and M. Plischke, Phys. Rev. E **59**, 2578 (1999).

[22] A. Vilfan, E. Frey, and F. Schwabl, Europhys. Lett. **45**, 283 (1999).

[23] Z. Csahók, F. Family, and T. Vicsek, Phys. Rev. E **55**, 5179 (1997).

[24] D. Dan, A. M. Jayannavar, and G. I. Menon, Physica A **318**, 40 (2003).

[25] K. T. Forest and J. A. Tainer, Gene **192**, 165 (1997).

[26] H. Sun, D. R. Zusman, and W. Shi, Curr. Biol. **10**, 1143 (2000).

[27] J. M. Skerker and H. C. Berg, Proc. Natl. Acad. Sci. USA **98**, 6901 (2001).

[28] S. Krause, M. Bárcena, W. Pansegrouw, R. Lurz, J. M. Carazo, and E. Lanka, Proc. Natl. Acad. Sci. USA **97**, 3067 (2000).

[29] K. T. Forest, K. A. Satyshur, G. A. Worzalla, J. K. Hansen, and T. J. Herdendorf, Acta Crystallogr. D **60**, 978 (2004).

[30] N. LeBrasseur, J. Cell Biol. **159**, 912a (2002).

[31] D. Kaiser, Curr. Biol. **10**, R777 (2000).

[32] S. Klumpp, A. Mielke, and C. Wald, Phys. Rev. E **63**, 031914 (2001).

[33] P. E. Kloeden and E. Platen, *Numerical Solution of Stochastic Differential Equations* (Springer Verlag, 1992).

[34] R. D. Astumian, Science **276**, 917 (1997).